UCRL- 96363
PREPRINT

SHOCK STRENGTH VERSUS RANGE FROM UNDERWATER NUCLEAR EXPLOSIONS

Carl E. Rosenkilde

This Paper was Prepared for Submittal to:
The DNA Workshop on Hydrocode Application
in Ocean Environment
RDA, Marina del Rey, CA
January 14, 1987

January 27, 1987

DISCLAIMER

SHOCK STRENGTH VERSUS RANGE FROM UNDERWATER NUCLEAR EXPLOSIONS

UCRL--96363

DE87 008424

C. E. Rosenkilde

Lawrence Livermore National Laboratory

January 1987

ABSTRACT

Annotated viewgraphs describe the variation in pulse strength and duration as strong and weak spherical shock waves propagate through uniform, homogeneous water from a nuclear explosive source. Asymptotic relationships for strong and weak shocks are re-expressed in intrinsic non-dimensional units. These relationships are combined to obtain continuous interpolation formulas, which span the entire spatial range from the near-source region out through the far field of interest in submarine damage prediction. Comparisons are made between the semi-empirical results of Snay and some more recent hydrocode calculations by Kamegai.

This briefing was prepared for presentation at the DNA Workshop on Hydrocode Application in Ocean Environment, held at RDA, Marina del Rey, CA, 1/14/87.

----

*This work was performed under the auspices of the U.S. Department of Energy by Lawrence Livermore National Laboratory under contract No. W-7405-Eng-48.

LLNL EFFECTS-AT-SEA PROJECT

LLNL supported an investigation into nuclear weapon effects-at-sea during the four-year period from 7/79 to 9/83, as part of the Laboratory's contribution to Phase I and II studies for the SEALANCE system. The project involved several Laboratory personnel and a number of part-time academic consultants.

There were three general areas of concentration:

(1) Near source phenomena were investigated by means of hydrocode calculations in both one and two dimensions. The one-dimensional calculations[1] were designed to establish how well our available hydrocodes could recalculate the empirical information from the the WIGWAM event. Then three two-dimensional calculations[2,3] were done to investigate the irregular surface reflection of an underwater shock wave. Kamegai will describe his calculations later in this workshop.

(2) Theoretical investigations of weak-shock propagation and decay were conducted in one and two dimensions. The familar asymptotic pressure-range and pulse duration-range relationships for weak shocks in one dimension were reproduced[4] by extending an elementary method due to G. I. Taylor. However, our effort on two-dimensional interactions involving caustics was superseded by the work of Kuperman and McDonald.[5] The transition to purely acoustic pulse decay at much longer range was estimated by using methods described by Fridman.[6]

(3) Submarine damage assessment was investigated by means of a numerical model,[7] which was designed to bridge the gap between the elementary Murray model and the very detailed calculations with DYNA and other similar finite element codes. The model has been used to investigate angle-of-incidence effects.[8] The model was developed on a CDC-7600 and has been transferred to a VAX, but not yet to a CRAY.

This presentation will describe some aspects of items (1) and (2) which are applicable to hydrocode validation.

EARLY-TIME PHENOMENA

A multitude of different phenomena occur on different time scales in connection with underwater nuclear explosions. We have arbitrarily categorized as early-time phenomena, those things which have characteristic time scales on the order of microseconds, milliseconds, and seconds, and which primarily affect damage predictions.

A multitude of phenomena affect tactical performance

Early–time phenomena affect damage

Microseconds:

- Radiation deposition

Milliseconds:

- Shock front formation and propagation
- Formation of micro bubbles

Seconds:

- Bubble oscillation
- Cavitation
- Surface waves

Fig. 1

LATE-TIME PHENOMENA

Late-time phenomena, which have time scales on the order of minutes and hours, leave the environment in a disturbed state and may affect target detection for a similar period of time. Residual radioactivity and other environmental effects, which may persist to much longer time scales, will not be discussed further here.

A multitude of phenomena affect tactical performance (cont.)

Late–time phenomena affect detection

Minutes:

- Bubble rise
- Surface pool formation
- Convective flow and mixing
- Internal waves
- High–frequency reverberation

Hours:

- Thermal diffusion
- Low–frequency reverberation

Fig. 2

RADIATION DEPOSITION ISSUES

Let us assume that an nuclear explosion has taken place deep underwater. On a very short time scale of the order of microseconds or less, all the energy from the device is released. This output, a large fraction of which consists of neutrons and photons, is deposited in the immediate vicinity of the explosion.

This figure illustrates the mass attenuation coefficients for photons in water as a function of photon energy. The product of the total attenuation coefficient and the density of water gives the reciprocal of the mean free path. These mean free paths in water are on the order of 50 centimeters or less for all of the photon energies of interest. The mean free paths of all of the slow explosion products, e.g. neutrons and charged particles, also are short.

Ref.: R. D. Evans, The Atomic Nucleus, (McGraw-Hill Book Company, Inc., N. Y., 1955) p. 714.

Mass attenuation coefficients for photons in water

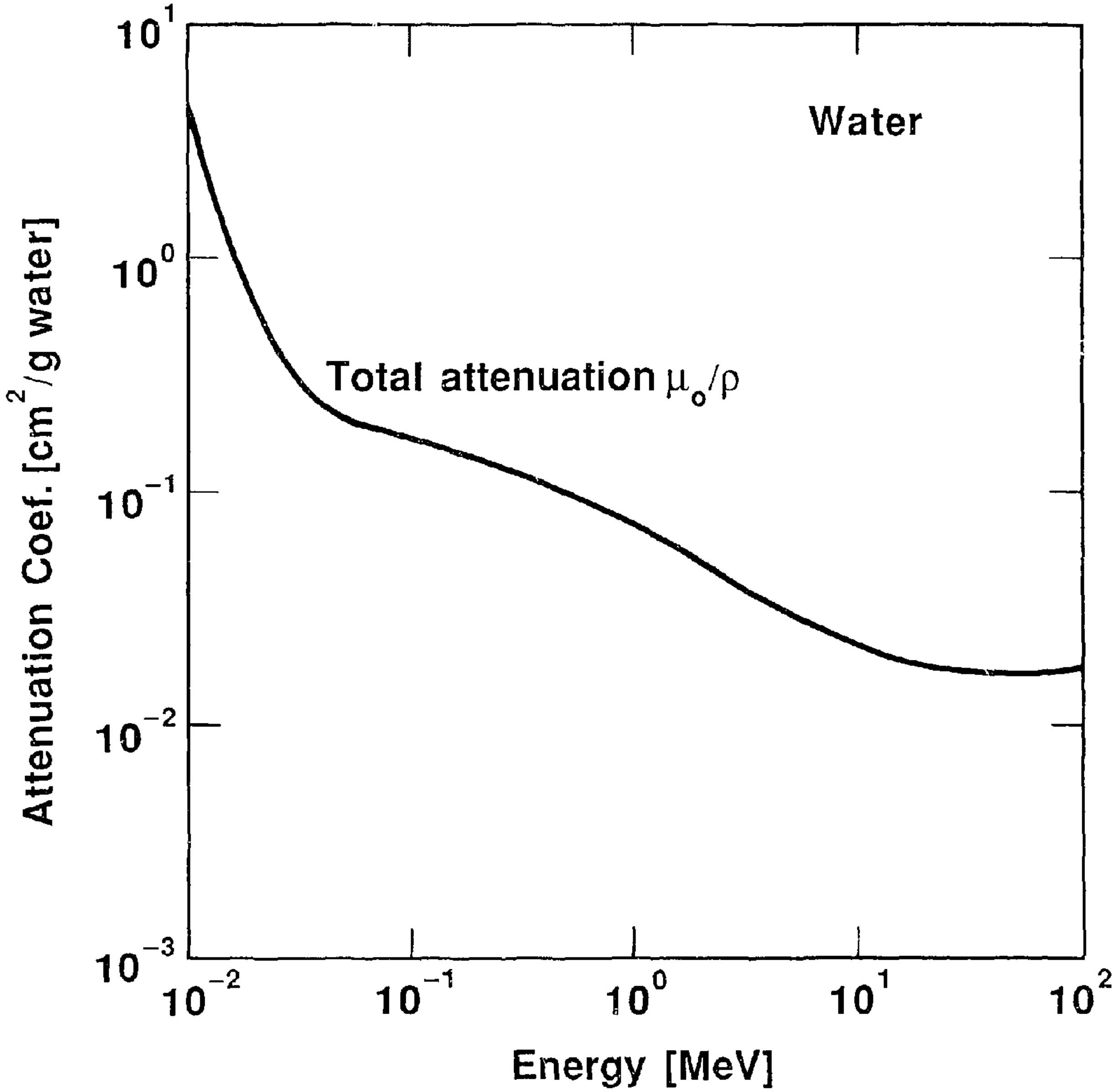

Photon Energy	m.f.p. in water
10 keV	0.25 cm
100 keV	6 cm
1 MeV	15 cm

Fig. 3

ESTIMATES OF INITIAL EXPLOSIVE OVERPRESSURE

It is interesting to compare the initial overpressure which is generated by a conventional chemical explosive (TNT) with that generated in a nuclear explosion.

An estimate of this pressure can be obtained by using the fact that pressure is a measure of energy density, the amount of energy contained in a unit volume of space. These quantities have the same dimensions, but different units. One Pascal is a Newton per square meter, which is equivalent to a Joule per cubic meter.

In the case of TNT, assume that the density is 1.6 grams per cc and that 1100 calories are released per gram. Then the corresponding energy density, expressed as a pressure, is 70 kilobars. This estimate is independent of the size and weight of the explosive charge; piling on more explosive does not generate a higher initial overpressure.

In the case of nuclear explosions, let us use the fact that there exist nuclear artillery shells to guess a size. If 1 Kt of energy is released within a sphere with a radius of 10 cm, the initial energy density, when converted to units of pressure, is 10,000 Megabars. This is more than 100,000 times that obtained with chemical explosives.

Estimates of initial explosive overpressure

Pressure ~ energy/volume

I. Conventional chemical explosion (TNT)

density ~ 1.6 g/cm^3; 1100 cal/g released

$$\text{energy density} \sim \frac{1.6\ \text{g}}{(10^{-2}\ \text{m})^3} \cdot 1100\ \frac{\text{cal}}{\text{g}} \cdot 4\ \frac{\text{J}}{\text{cal}}$$

$$\sim 7 \cdot 10^9\ \frac{\text{J}}{\text{m}^3} \sim 7 \cdot 10^9\ \text{Pa} \sim 7 \cdot 10^4\ \text{bar} \sim 70\ \text{kbar}$$

Independent of size or weight!

II. Nuclear explosion

8 in. ~ 20 cm diameter; 1 kt ~ $4 \cdot 10^{12}$ J

$$\text{energy density} \sim \frac{4 \cdot 10^{12}\ \text{J}}{\frac{4\pi}{3}(10^{-1}\ \text{m})^3} \sim 10^{15}\ \frac{\text{J}}{\text{m}^3}$$

$$\sim 10^{15}\ \text{Pa} \sim 10^{10}\ \text{bar} \sim 10^4\ \text{Mbar}$$

Fig. 4

SCHEMATIC PRESSURE-TIME HISTORY

The shock wave generated by an underwater explosion will be attenuated as it propagates through the water. Damage to submarines can be inflicted even at long range from the explosion. Damage levels for submarines are often characterized by the amount of peak translational velocity (PTV) or the amount of (excess) impulse imparted to the submarine. These quantities require a knowledge of the peak overpressure and some measure of the pulse duration. The pulse shape often is approximated as a decaying exponential with a very short (in comparison) rise-time. The figure illustrates schematically a common way to define these quantities, which are a function of slant range, R. An approximate time scale can be extracted from the semi-logarithmic plot, even if the pulse does not decay as an exact exponential.

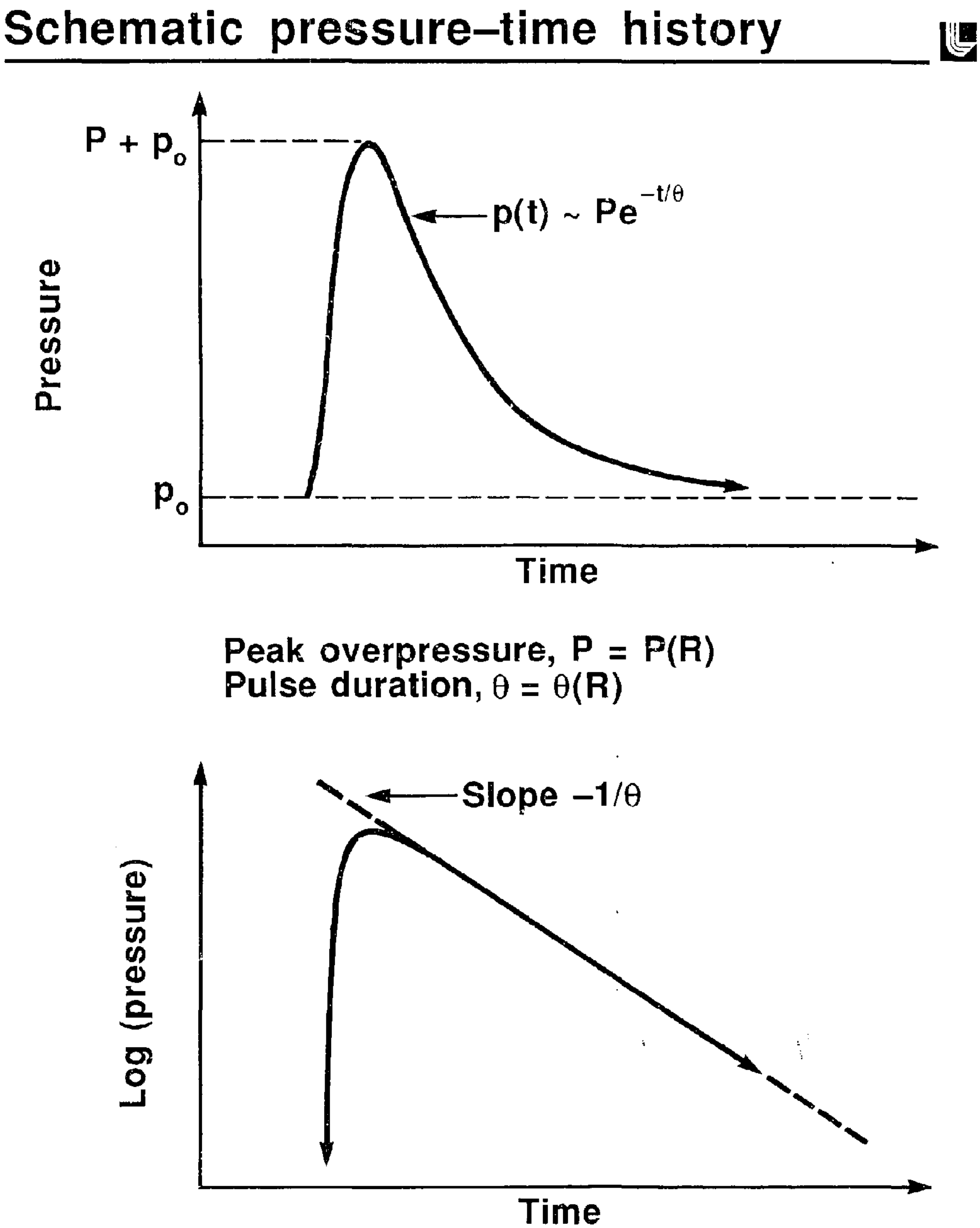

Schematic pressure–time history
P + p_o
p(t) ~ Pe^{-t/θ}
Pressure
p_o
Time
Peak overpressure, P = P(R)
Pulse duration, θ = θ(R)
Slope −1/θ
Log (pressure)
Time

Fig. 5

NUCLEAR SHOCK-WAVE PARAMETERS

The peak overpressure and pulse duration are functions of the slant range to the target and the yield of the explosive source. Typical values for these quantities can be obtained from this figure. Each family comprises curves for yields of 1 to 1000 Kt. The curves are based upon empirical data.

Nuclear shock–wave parameters

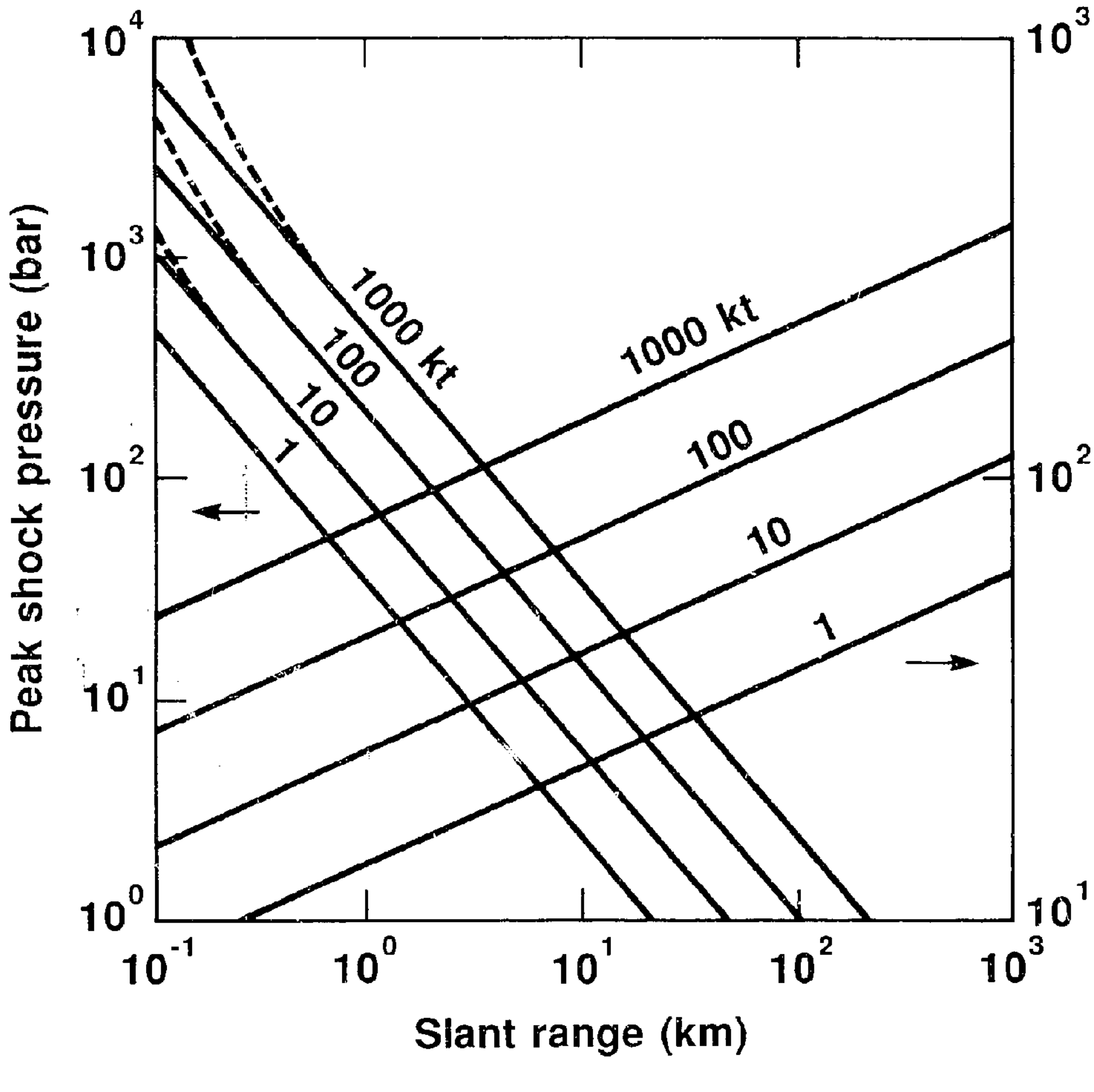

Fig. 6

PEAK OVERPRESSURE VERSUS RANGE IN WATER

There is interest in hydrocode calculations which begin with extremely high pressures in the source region and progress as far as possible down to overpressures of interest for submarine damage. The figure portrays the variation of peak shock overpressure as a function of slant range from an underwater nuclear explosion. Three different regimes are evident.

In the first regime very near the source, the very high initial overpressure decreases rapidly as the shock wave expands. The reduction in amplitude is proportional to the inverse cube of the distance from the point source. This regime is known as the strong shock or blast-wave regime. It was studied in the 1940's by Taylor, Sedov, and others, who obtained theoretical solutions to the hydrodynamical equations, by assuming that the disturbance is so strong that ambient conditions can be neglected. Then the pressure is proportional just to the total energy density within the expanding sphere.

At a certain characteristic distance, the rate of reduction in overpressure makes a transition to a second, more slowly varying regime. In this second regime, which is known as the weak shock regime, the overpressure decays slightly faster than the inverse power of the distance, and persists for a long distance. The pressure variation with distance in this regime is a consequence of the fact that the propagating disturbance is still a shock wave (and therefore, still is dissipating energy at the shock front) even though it is propagating with nearly the acoustic velocity. The transition to the third regime, of strictly acoustic propagation, occurs at a much greater distance, if it occurs at all.

The scales in this figure are logarithmic, and are expressed in terms of certain characteristic physical units, which are intrinsic to explosively driven shock waves in uniform materials.

Peak overpressure vs slant range

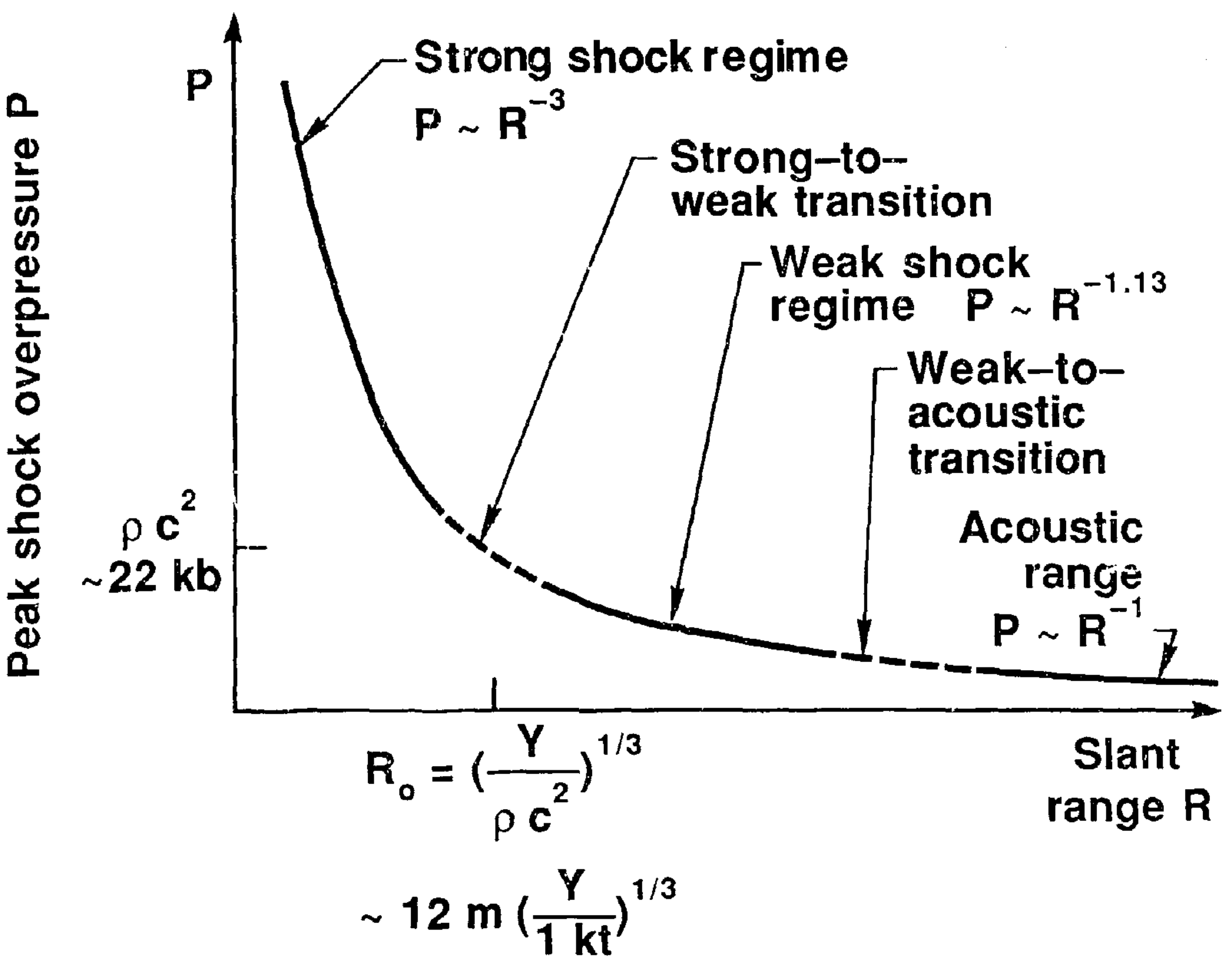

Fig. 7

CHARACTERISTIC PHYSICAL QUANTITIES

There is a set of characteristic physical quantities that are intrinsic to explosively driven shock waves in material media. Take as given fundamental properties or quantities, the total energy released by the explosion, the sound velocity of the ambient medium in which the explosion occurs, and the ambient density of this medium, rather than simply mass, length, and time. All other characteristic scales of interest can be constructed (derived) from these three given quantities.

A characteristic pressure, which is associated with the elastic properties of the medium and its ability to propagate elastic waves, is the adiabatic bulk modulus. It is the product of the density and the square of the sound speed. Since pressure times volume is an energy, a characteristic length can be constructed by taking the cube root of the ratio of the total energy and this pressure. A characteristic time scale can be obtained by dividing this length by the sound speed. The figure gives the order of magnitude of these scales in the case of a one kiloton energy release in water. Other characteristic physical scales of interest, such as those for acceleration, impulse per unit area, and energy flux, also can be constructed.

When these intrinsic scales are used to nondimensionalize other quantities of interest, such as overpressure and range, several important facts emerge. Firstly, the transition from strong to weak shock propagation occurs (see the previous figure) when both the overpressure and slant range are on the order of unity in these units. Secondly, this transition distance of approximately 12 $m/(Kt)^{1/3}$ occurs relatively close to the source, even for very large yields. This means that the disturbance propagates as a <u>weak shock</u> over most of the distance to the target. Thirdly, the overpressure expressed in these units is commonly known as the shock strength. Its magnitude has an important bearing on the suitability of hydrocodes.

Characteristic physical quantities

Density of $H_2O \sim \rho \sim 1$ gm/cm^3

Velocity ~ sound speed ~ $c \sim 1.5$ m/ms

Pressure ~ adiabatic bulk modulus ~ $B_o = \rho c^2 \sim 22$ kbar

Energy ~ yield ~ $Y \sim 1$ kt

Radius ~ $(\text{volume})^{1/3} \sim \left(\frac{\text{energy}}{\text{pressure}}\right)^{1/3}$

$$\sim R_o = \left(\frac{Y}{\rho c^2}\right)^{1/3} \sim 12 \text{ m}$$

Time ~ $\frac{\text{radius}}{\text{velocity}} \sim \theta_o = \frac{1}{c}\left(\frac{Y}{\rho c^2}\right)^{1/3} \sim 8$ ms

Fig. 8

ASYMPTOTIC OVERPRESSURE VERSUS RANGE IN WATER

Peak overpressure is proportional to some power of the range, within each of the two regimes of strong and of weak shocks. These power-laws assume particularly simple forms when they are expressed in terms of an appropriate set of characteristic scales. In fact the nondimensional decimal coefficients and exponents can be further approximated by simpler rational numbers for the purpose of rough extimates.

The power-law forms are represented in the figure by the dotted straight lines. The crosses represent a prediction, which was made by Snay, who used both empirical and numerical methods to obtain his results. The weak-shock relationship is based upon empirical data. The fact that the exponent of 1.13 in this regime is slightly greater than unity, indicates that the propagation still is nonlinear, and not strictly acoustic.

While power-laws may be adequate representations in the asymptotic realms of each of the two regimes, there is a transition region between the two regimes, which is not well-represented by any power-law. However, it is possible to construct an elementary interpolation formula to represent the overpressures in this transition region by simply adding the two asymptotic power-laws. This precedure generates the solid curve in the figure.

Ref.: H. G. Snay, J. F. Butler, and A. N. Gleyzal, "Predictions of Underwater Explosion Phenomena," in Operation WIGWAM, Project 1.1, Explosives Research Department, U. S. Naval Ordnance Laboratory Report, WT-1004(NOLR-1213), Jan. 24, 1957.

Asymptotic peak overpressure versus range

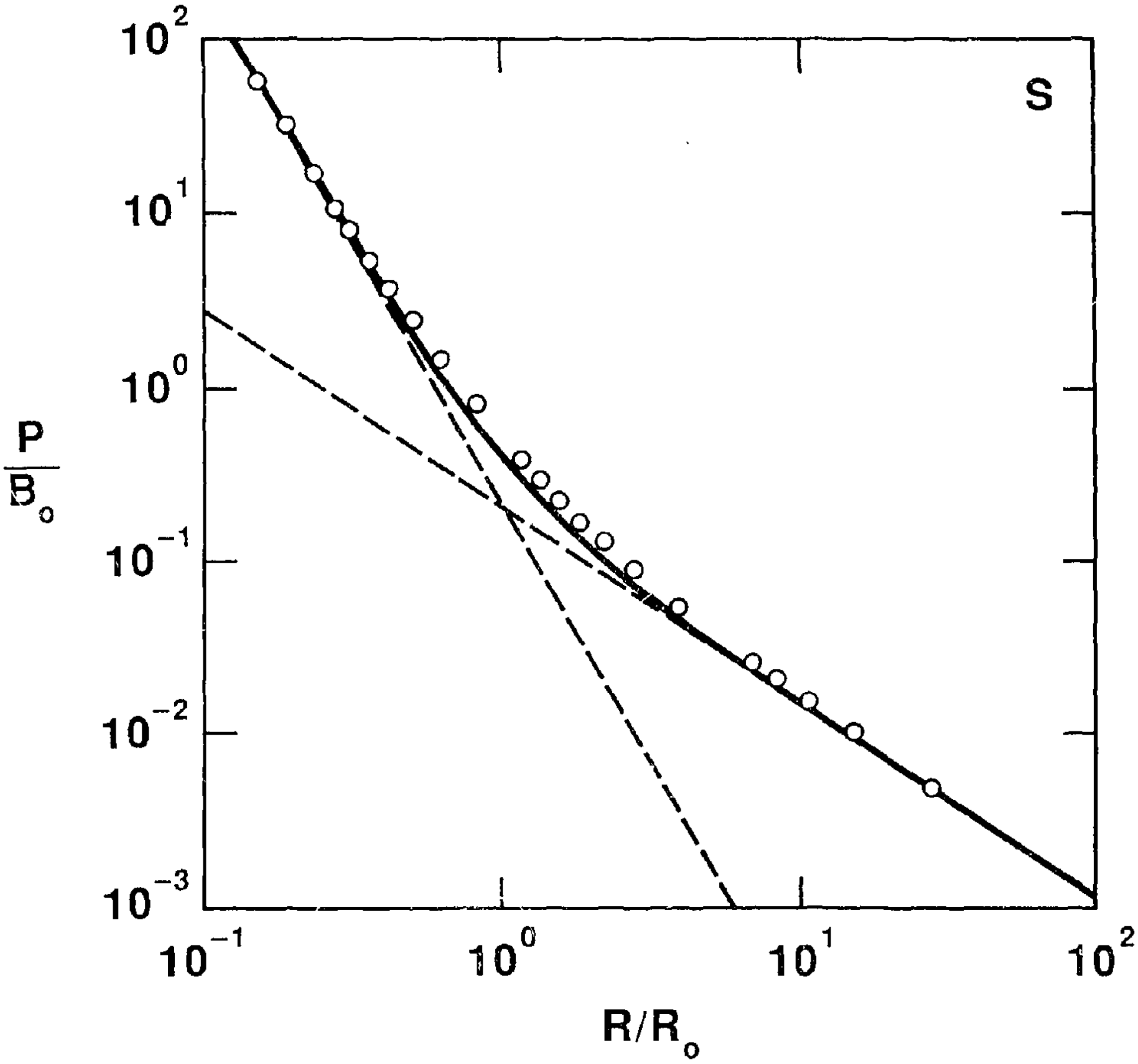

B_o = 22.54 kbar, $R_o = 12.29\ Y^{1/3}$ m/(kt)$^{1/3}$

Weak shock: $P/B_o = 0.2055\ (R_o/R)^{1.13} \sim 1/5\ (R_o/R)^{9/8}$

Strong shock: $P/B_o = 0.2122\ (R_o/R)^{3} \sim 1/5\ (R_o/R)^{3}$

For simple interpolation, use the sum: ———

Fig. 9

ASYMPTOTIC PULSE DURATION VERSUS RANGE

The pulse duration also is proportional to some power of the range, within each of the two regimes of strong and of weak shocks. In the strong blast-wave regime the pulse duration is proportional to the 5/2 power of the range. In the weak shock regime the pulse duration is known empirically to be proportional to the range raised to the power 0.22. Again, the fact that this quantity does not remain a constant as predicted by acoustics, indicates that the propagation has not reached the linear acoustic regime.

The pulse duration, θ, has been nondimensionalized in terms the intrinsic characteristic time scale, $\theta_o = R_o/c_o$. The coefficients and exponents can be rationalized for the purpose of rough estimates. Note that the relationships are expressed as reciprocals! This choice permits the construction of an elementary interpolation formula to represent the pulse duration in the transition regime, by simply adding the two reciprocals to obtain an estimate of the reciprocal of the overall pulse duration.

Asymptotic pulse duration versus range

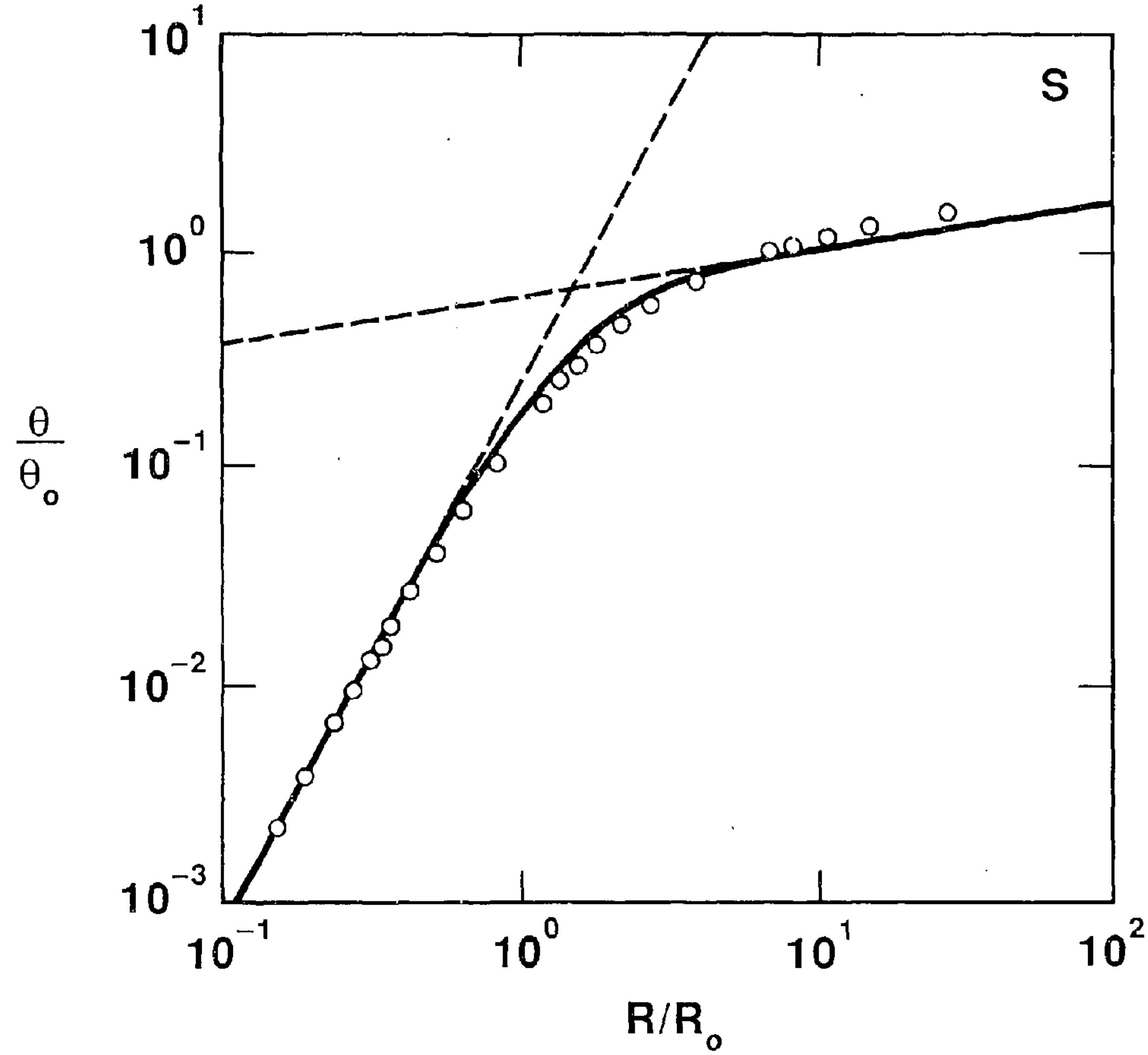

$R_o = 12.29\ Y^{1/3}\ m/(kt)^{1/3}$, $\theta_o = 8.287\ Y^{1/3}\ ms/(kt)^{1/3}$

Weak shock: $\theta_o/\theta = (0.6189)^{-1}\ (R_o/R)^{0.22} \sim 5/3\ (R_o/R)^{2/9}$

Strong shock: $\theta_o/\theta = (0.2409)^{-1}\ (R_o/R)^{5/2} \sim 4\ (R_o/R)^{5/2}$

For simple interpolation, use sum (of reciprocals!): ——

Fig. 10

THREE-TERM INTERPOLATION FORMULA FOR OVERPRESSURE

The two-term interpolation formula, which was constructed by simply adding the asymptotic power-law formulas for strong and weak shocks, underestimates the peak overpressure in the transition region which is in the neighborhood where the overpressure and range assume their characteristic values.

This situation can be rectified by re-fitting (in the least-square sense) Snay's points to a three-termed formula. (Three-termed formulas, due to Brode, have long been used for estimates of airblast.) Such a formula has been constructed by accepting as given, the exponents -3 and -1.13 for the asymptotic regimes, and introducing a third term with an exponent, which has an arbitrarily chosen value of -2, that is intermediate between these two extremes. New coefficients for all three terms then are obtained by a least-squares fitting procedure. Notice that the value of the coefficient in front of the long-range term (with the exponent of 1.13) changes by less than 1% (from 0.2055 to 0.2041). (There is less than a 10% change in the coefficient on the relatively unimportant short-range term.)

This three-termed interpolation formula represents the iso-velocity free-water peak-overpressure versus range relationship for deep underwater nuclear explosions adequately enough for most practical estimates down through the domain of interest in connection with submarine damage. The uncertainty is between 10 and 20 percent. (However, it does not pretend to account for the effects of surface rarefaction, bottom reflection, nor refraction.)

This interpolation formula can be used as a benchmark (or calibration) against which to compare how well hydrocodes, which are optimized for very high pressure regimes, can access the low-pressure weak-shock regime.

3–term interpolation of P vs R

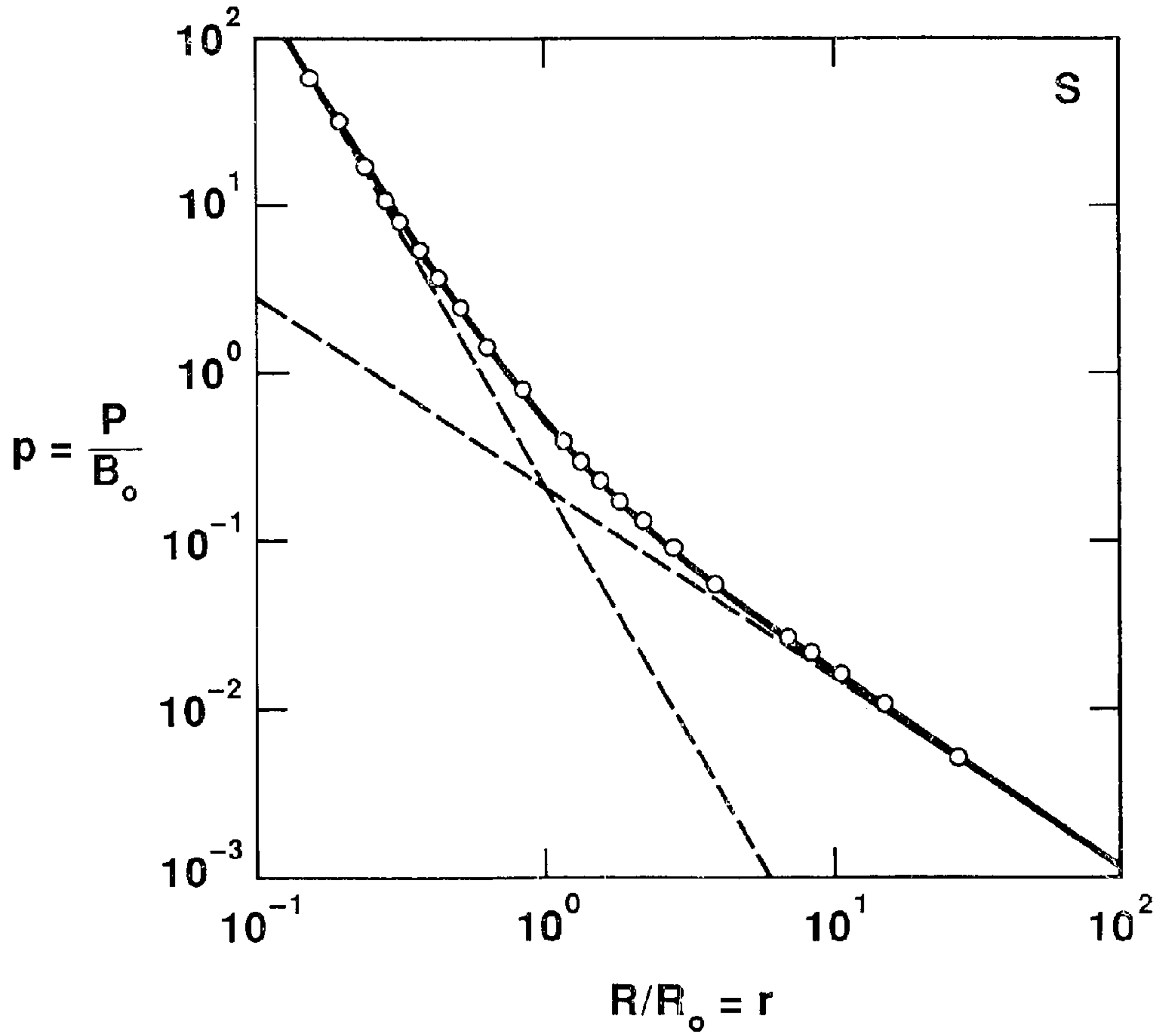

B_o = 22.54 kbar, $R_o = 12.29\ Y^{1/3}\ m/(kt)^{1/3}$

$p = 0.1933\ r^{-3} + 0.1393\ r^{-2} + 0.2041\ r^{-1.13}$

Fig. 11

THREE-TERM INTERPOLATION FORMULA FOR PULSE DURATION

Similar arguments can be used to construct a three-termed interpolation formula for pulse duration versus range. In this case we accept as given, the exponents of -5/2 and -0.22 for the asymptotic regimes, and introduce an intermediate term with an exponent of -3/2. New coefficients for all three terms then can be determined by a least-squares fitting procedure. [It is not known why Snay's points exceed the empirical fit (dashed line) by about 12% in the weak-shock regime, and in fact upon closer inspection appear to be following a line with a greater slope closer to 0.3.]

This three-termed interpolation formula represents the iso-velocity free-water pulse-duration versus range for deep underwater nuclear explosions adequately enough for most practical estimates down through the domain of interest in connection with submarine damage. [However, there is more uncertainty associated with this fit than there is with peak overpressure (c.f., Petukhov).]

The two interpolation formulas for overpressure and for pulse duration provide enough information about the wave shape to estimate integral quantities, such as impulse and energy-flux, as a function of range. They also could be used to generate representative waveforms near the transition regime to be used as initial conditions for purely weak-shock propagation codes.

Ref.: Yu. V. Petukhov, "Interpretation of the Anomalous Behavior of the Pressure Waveform from an Underwater Explosive Source," Sov. Phys. Acoust. 29(2), 142-144, Mar.-Apr. 1983.

3–term interpolation of θ vs R

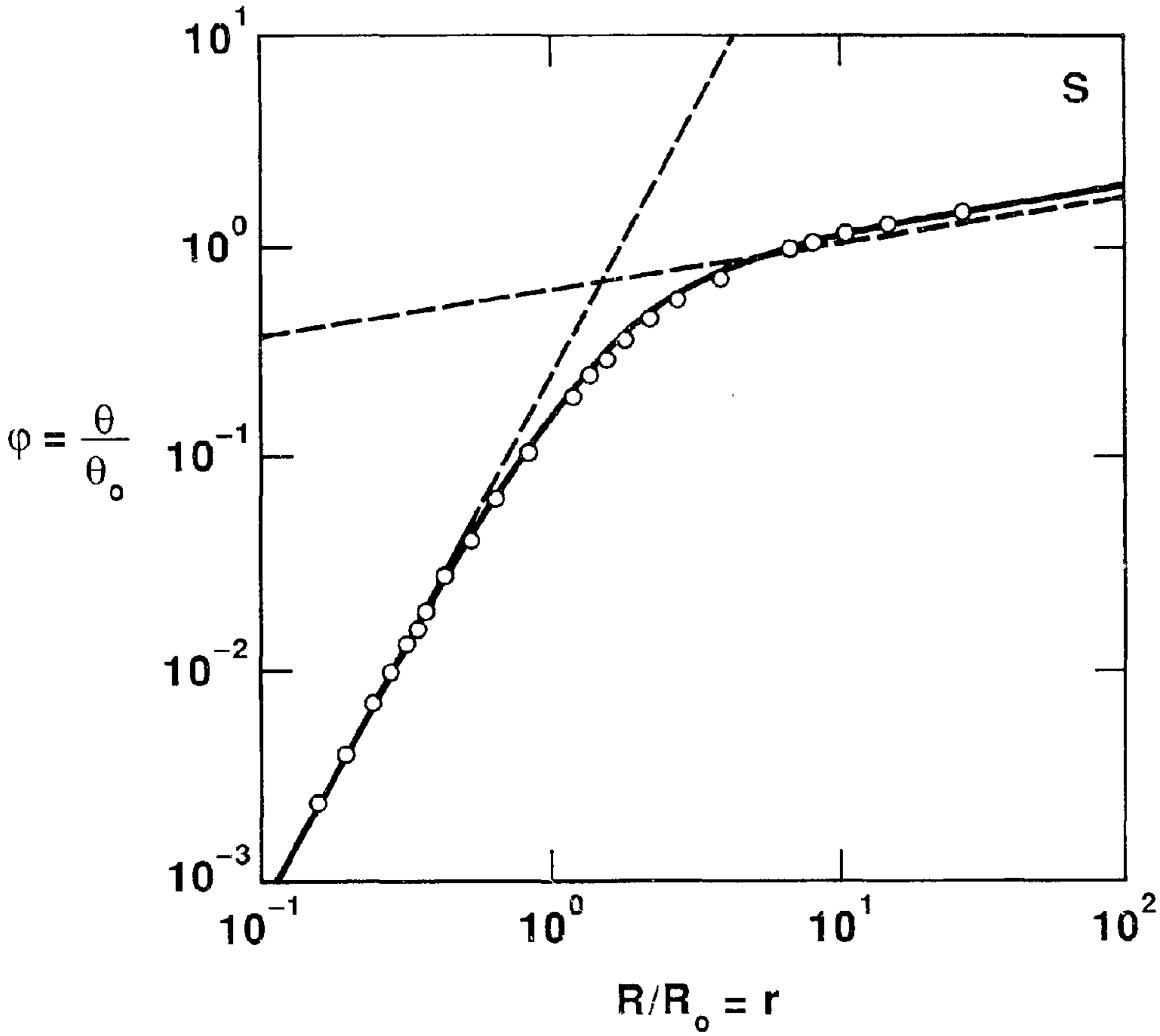

$$\theta_o = 8.287\ Y^{1/3}\ \text{ms/(kt)}^{1/3},\ R_o = 12.29\ Y^{1/3}\ \text{m/(kt)}^{1/3}$$

$$\varphi^{-1} = (0.2420)^{-1}\ r^{-5/2} + (0.8826)^{-1}\ r^{-3/2} + (0.7072)^{-1}\ r^{-0.22}$$

Fig. 12

DAMAGE CRITERIA

This figure has been designed to show the connection between peak shock overpressure and conventional damage criteria for submarines. Without elaborating too much on the details, let us remark that the survivability of a submarine hull often is correlated with the amount of excess impulse (XIMP) it receives. (This is the time integral of the shock pressure exceeding the difference between the hydrostatic pressure and the collapse pressure.) Interesting values of this quantity are in the range of a few tens of psi-s. Safe standoff from an explosion often is correlated with the peak translational velocity (PTV) imparted to the hull by the enveloping shock wave. Interesting values of the quantity are in the range of a few ft/s.

The curves shown in the figure have been calculated by using a crude model to relate these damage criteria to peak shock overpressure. The figure shows that hull crush may occur at overpressures above a few hundred bar, while safe standoff may be possible below overpressures of a few tens of bars. Since the characteristic overpressure is on the order of 20 Kbar for shocks in water, it follows that the interesting range for shock strength is in the range of 10^{-2} to 10^{-3}. The corresponding values of the nondimensional range are 20 to 200, which are approximately 1/5 of the reciprocals of the respective shock strength in this regime. The actual ranges then are found by multiplying by the characteristic range, which is on the order of 10 (actually 12.5) $m/Kt^{1/3}$.

Damage criteria

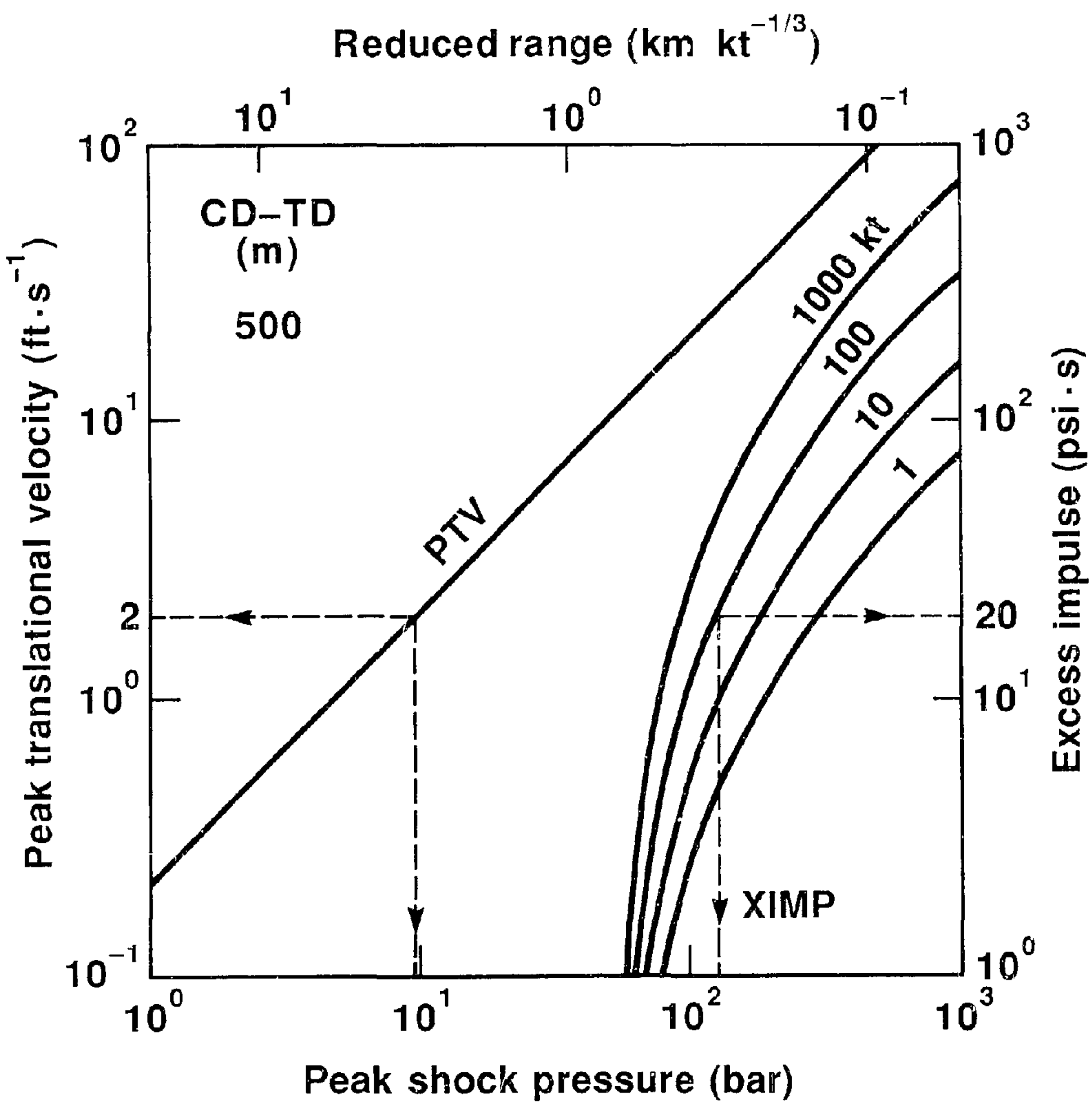

Fig. 13

DOMAIN OF VULNERABILITY

On the basis of the foregoing estimates, it is possible to identify a domain of interest in the case of submarines . In this plot of nondimensional peak overpressure versus nondimensional range, the domain of interest lies in the lower right-hand corner. The rectangle shown in the figure is well out into the weak-shock regime. The size of this rectangle depends upon the connection between overpressure (and range) and some levels of damage, which are described crudely here as crush and survive.

If this same curve is regarded in some sense as universal and applicable also to airblast, then the corresponding rectangle will fall slightly above and to the left of center in the figure. In this case the domain of interest is in the strong-shock regime.

In the case of underground shock waves incident on harder targets, this rectangle is located in the same neighborhood of the weak-shock overpressure regime as that for the case of water, because both the "hardness" and the bulk moduli increase by comparable factors in that case. However, the corresponding ranges are somewhat less because porous ground is more dissipative to propagating shocks.

These considerations have a direct bearing upon the choice (and ultimate success) of calculational techniques that might be utilized to traverse any significant portion of the range from source to target!

Domain of vulnerability

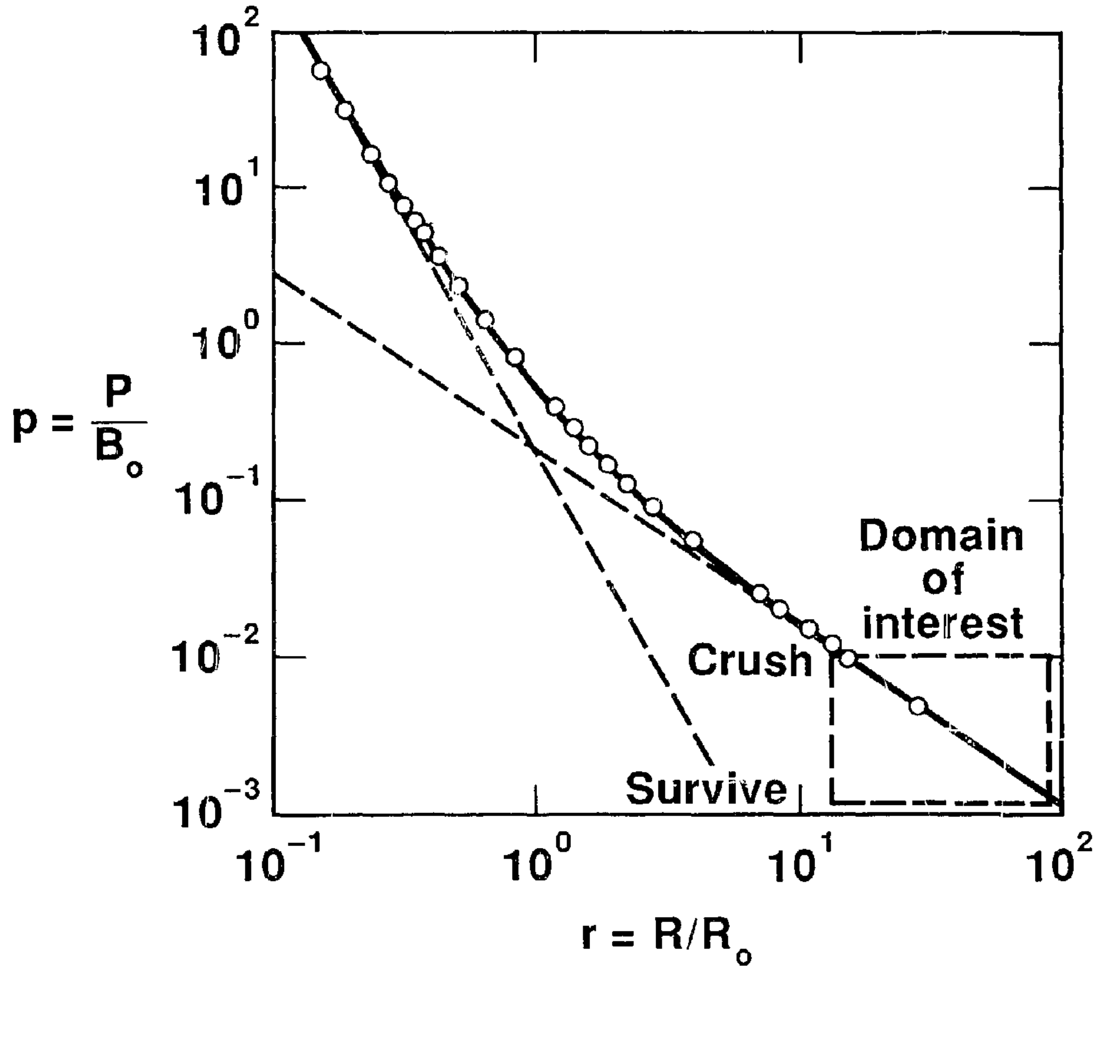

Fig. 14

WEAK SHOCK VERSUS ACOUSTIC PROPAGATION

A great deal of effort has been spent in establishing the appropriate exponent to be used in the power law for overpressure versus range. Is the increment of 0.13 over unity really that important? Wouldn't a prediction, which is based upon the acoustic 1/r dependence, do just as well?

This issue can be explored by estimating the fractional difference in overpressure that would be predicted by these two different power laws, if they were in general agreement initially at the point (1,1) in nondimensional units. There is an 82% difference by the time the disturbance has propagated to interesting distances, and a 145% difference by the time the disturbance begins to surpass the interesting distances. Even greater differences obtain if the disturbance should happen to decay more like a cylindrical, rather than spherical, wavefront. (Weak shock theory predicts a cylindrical wave amplitude to decay as the inverse 3/4 power of the range. Spherical waves have a logarithmic factor in addition to the inverse range. [c.f., Whitham])

All this simply means that care must be taken in applying the results of acoustics to problems of this sort. The Mach number differs from unity by the shock strength, which is of the order of 10^{-3}. Nevertheless, the disturbance still is a shock wave, and therefore, must be dissipating energy at a very small rate at the shock front. Fridman [Ref. 5] has argued that if the effects of nonlinear convection (steepening) are balanced by the various dissipative effects (rounding), the disturbance will continue to propagate as a steady wave to a much greater distance.

Ref.: G. B. Whitham, Linear and Nonlinear Waves, (John Wiley & Sons, New York, 1974), p. 322.

Weak shock vs acoustic propagation or does an exponent of 0.13 really matter?

$$\frac{P_s}{B_o} = A_s \left(\frac{R_o}{R}\right)^{1.13}$$

$$\frac{P_A}{B_o} = A_A \left(\frac{R_o}{R}\right)^{1}$$

$$\frac{P_c}{B_o} = A_c \left(\frac{R_o}{R}\right)^{3/4}$$

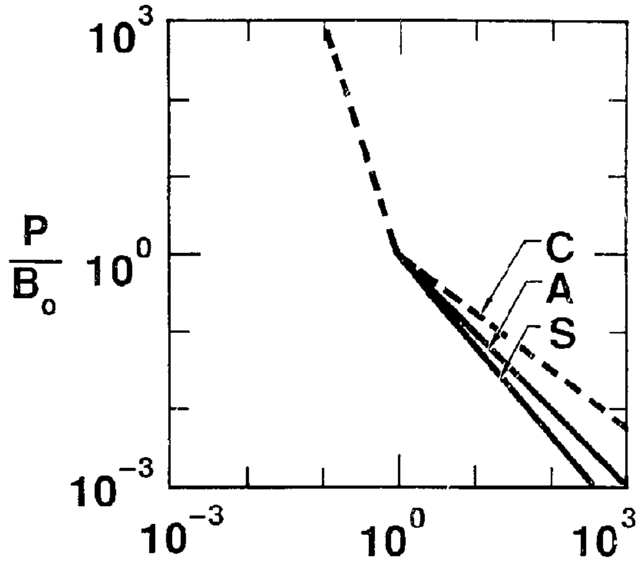

Suppose $P_S = P_A = P_C$ at $R = R_o \Rightarrow A_S = A_A = A_C$

Then

$$(P_A - P_S)/P_S = (R/R_o)^{0.13} - 1 \text{ and } (P_C - P_S)/P_S = (R/R_o)^{0.38} - 1$$

R/R_o	$\Delta P_A/P_S$	ΔP_C P_S
10	0.35	1.40
10^2	0.82	4.75
10^3	1.45	12.80

Fig. 15

COMPUTER SIMULATION OF UNDERWATER NUCLEAR EXPLOSIONS

Predictions of the peak overpressure and pulse duration associated with a shock wave, which has propagated out to some scaled slant range from a deep underwater explosion, can be made by using the foregoing interpolation formulas. However, these relationships really are appropriate only for the ideal situation of iso-velocity, homogeneous water with no interactions with interfaces, such as the surface or bottom. Much more uncertainty exists, if any of these restrictions are relaxed.

It would be desirable to model more complicated situations, particularly those which involve shock interactions or environmental gradients, by utilizing the computer. Direct simulation using hydrocodes is now feasible. The figure illustrates that various hydrocodes available at LLNL (in 1980) could be used to put points on various parts of the pressure versus range curve being discussed. However, no single hydrocode was able to cover the entire range of interest from source to target. The problem is that hydrocodes, which have been optimized to do very high pressure physics, do not propagate weak shocks efficiently, and vice versa.

Nevertheless, there was a need to investigate shock propagation away from a near-surface underwater nuclear explosion with available two-dimensional hydrocodes. Consequently, as a preliminary exercise before attempting any more complicated problem, it was essential to determine just how well these codes could reproduce the "known" pressure versus range in uniform homogeneous infinite water. Kamegai (Ref. 1) has described this calculation. The subsequent figures illustrate his results and show some comparisons.

Computer simulation of underwater nuclear explosions

LLNL, circa 1980

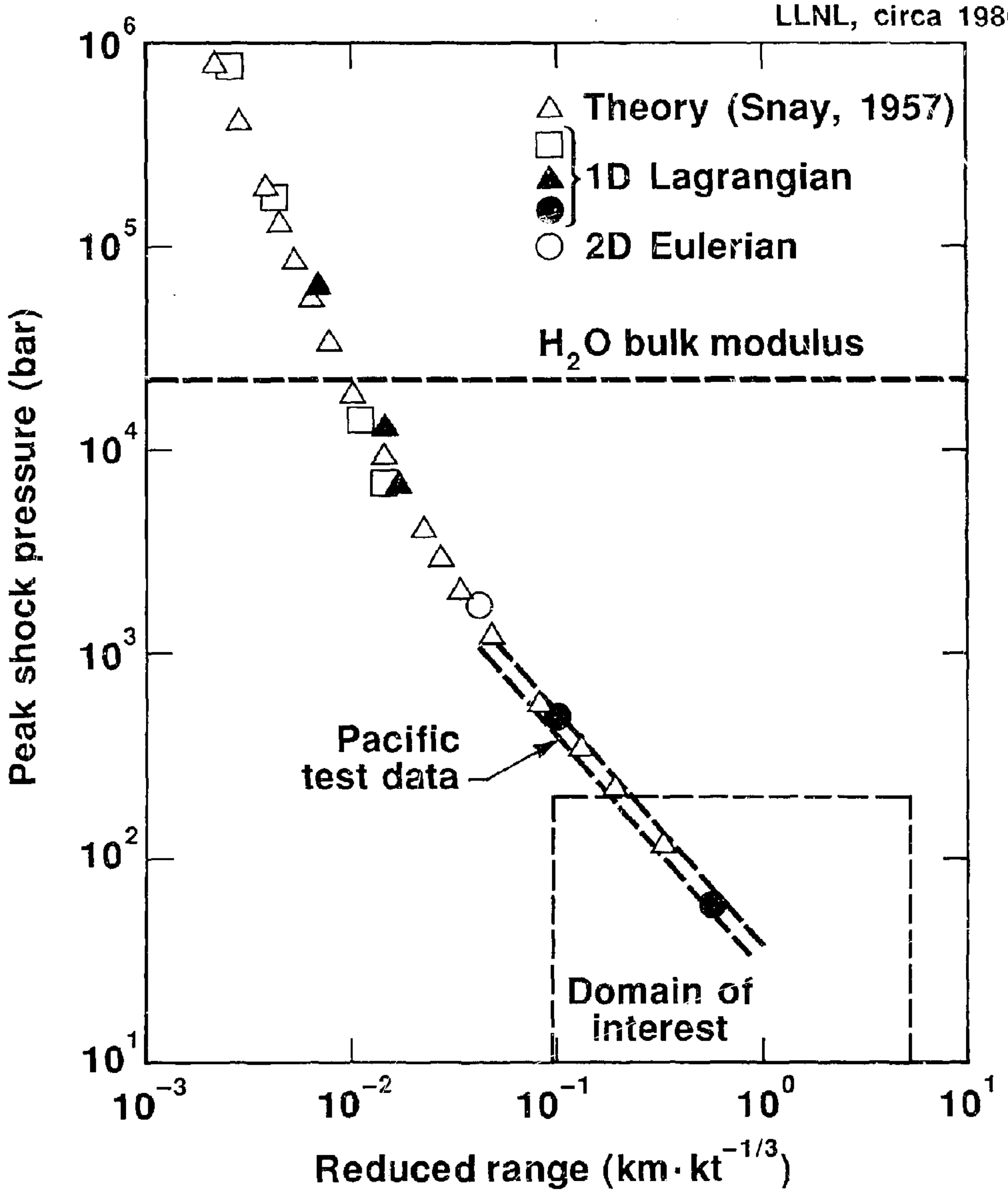

Fig. 16

COMPUTER SIMULATIONS WITH LASNEX

Two computer simulations of underwater explosions were carried out with LASNEX: (I) a simulation of the WIGWAM test, and (II) a simulation of a modern device of greater yield and radiative output. Kamegai (Ref. 1) has described some details and his results.

Selected points from these two simulations were fit by a least-squares procedure to three-termed functions utilizing the same sets of basis functions as were used earlier in fitting Snay's points. This figure illustrates the functions for peak overpressure versus range in nondimensional units. The curves are labeled in the figure: S for Snay, W for WIGWAM, and M for Modern. The corresponding formulas are:

$$p = 0.1933\ r^{-3} + 0.1393\ r^{-2} + 0.2041\ r^{-1.13}, \qquad (S)$$

$$p = 0.1857\ r^{-3} + 0.2741\ r^{-2} + 0.1683\ r^{-1.13}, \qquad (W)$$

$$p = 0.1920\ r^{-3} + 0.2112\ r^{-2} + 0.1675\ r^{-1.13}. \qquad (M)$$

It is to be noted that the asymptotic values for the coefficients here differ from those in our fit of the Snay points. In particular, both fits underestimate the overpressure, which is given by the Snay fit, by about 20% in the weak-shock limit.

Computer simulation of peak overpressure versus range

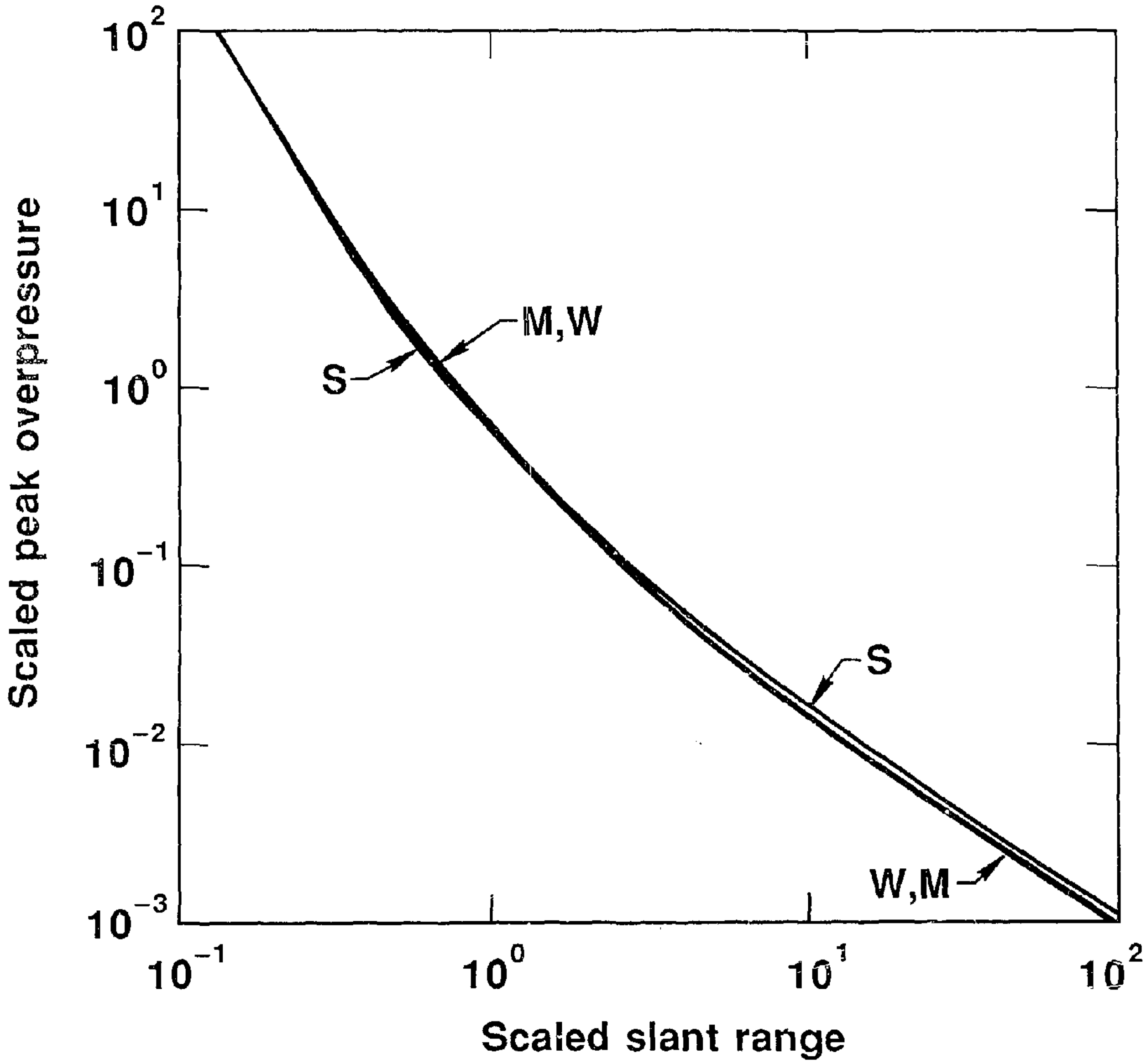

Fig. 17

COMPARISON OF PEAK OVERPRESSURES

This figure compares fits to Kamegai's two computer simulations with our fit to Snay points. Curve W is, the ratio of overpressure given by the foregoing fit to the WIGWAM simulation, to the overpressure given by the fit to the Snay points. Curve M is the corresponding ratio for the hypothetical modern device. These ratios are plotted against the corresponding Snay overpressure. (Note that the weak-shock regime now is on the left-hand side of the figure.)

This figure shows more clearly that the overpressures in both nuclear simulations fall about 20% below the Snay prediction in the weak-shock limit. Moreover, this underestimation begins around 1 Kbar overpressures, and becomes steadly worse for lower overpressures.

This underestimation of peak overpressure probably is not real. It is indicative of decreasing resolution due to artificial viscosity and to coarser zoning at longer range, and the fact that hydrocodes, which are optimized for high pressure physics in compressible media, do not operate efficiently at low pressures in nearly incompressible media.

Comparison of peak overpressures

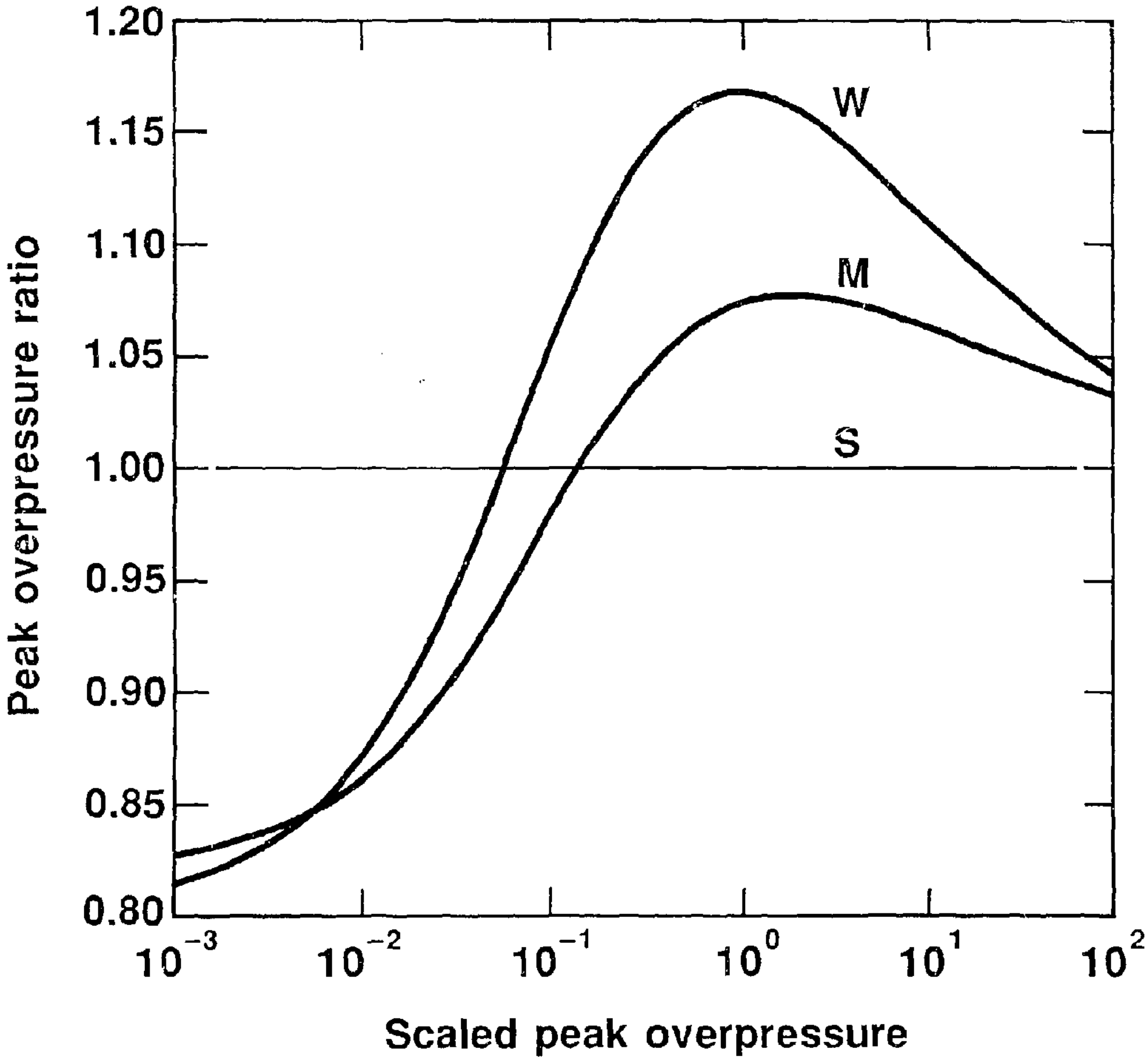

Fig. 18

COMPUTER SIMULATION OF PULSE DURATION VERSUS RANGE

Least-square fits to the estimated pulse durations from each simulation also have been constructed. The figure illustrates these fits, together with our fit to Snay's points. The curves are labeled in the figure: S for Snay, W for WIGWAM, and M for Modern. The corresponding formulas (in our nondimensional units) are:

$$1/\phi = 1/(0.2420\ r^{2.5}) + 1/(0.8826\ r^{1.5}) + 1/(0.7072\ r^{0.22}), \quad (S)$$

$$1/\phi = 1/(0.3751\ r^{2.5}) + 1/(0.4517\ r^{1.5}) + 1/(0.7341\ r^{0.22}), \quad (W)$$

$$1/\phi = 1/(0.4934\ r^{2.5}) + 1/(0.3278\ r^{1.5}) + 1/(0.7374\ r^{0.22}). \quad (M)$$

The computer simulations appear to significantly overestimate the Snay points at short range (high pressures).

Computer simulation of pulse duration versus range

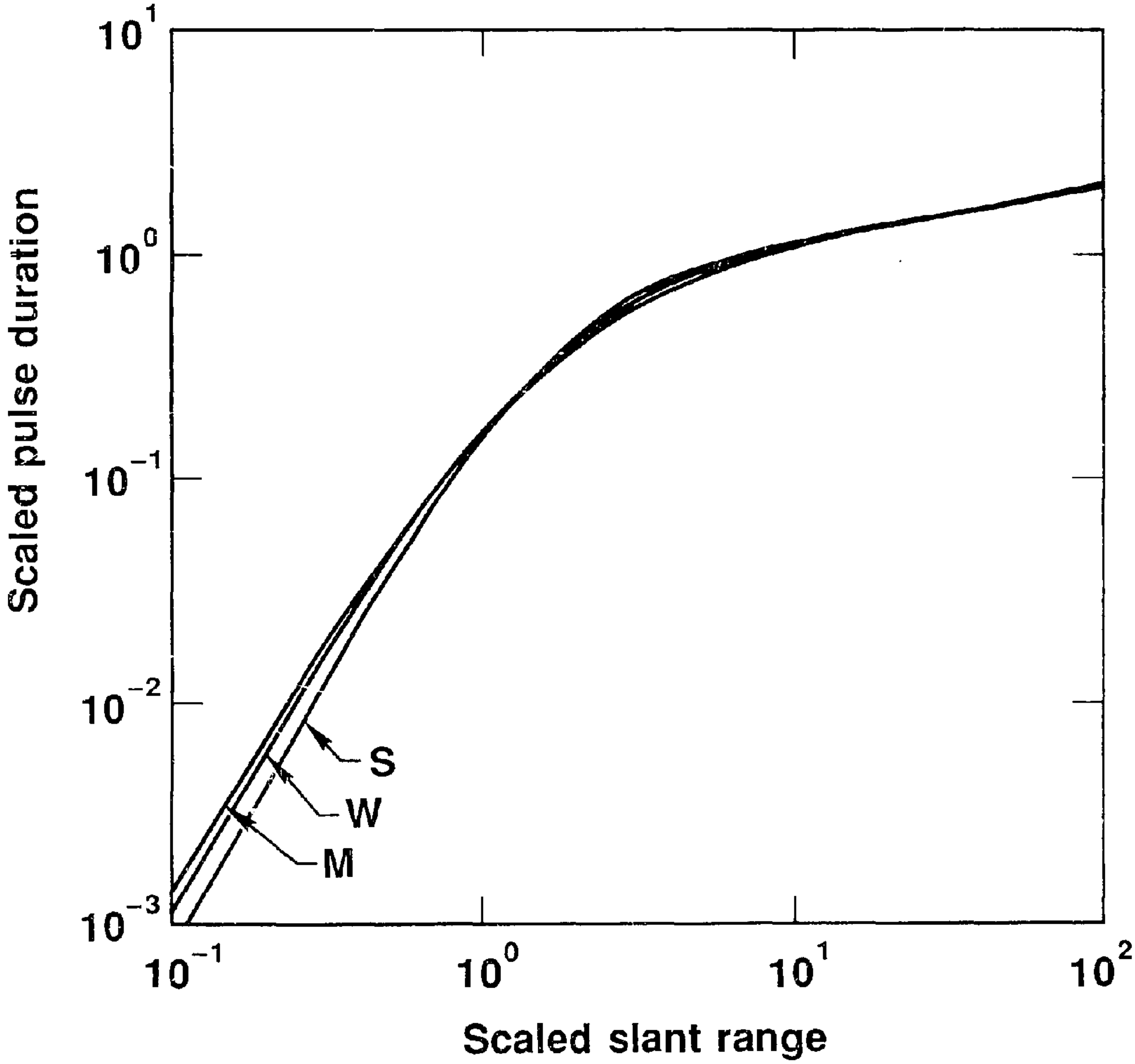

Fig. 19

COMPARISON OF PULSE DURATIONS

This figure compares fits to the two computer simulations with our fit to the Snay points. Again, the ratios of the pulse durations at corresponding ranges are plotted against the corresponding overpressure predicted by Snay.

This figure shows more clearly that the computer-simulated pulse durations are significantly greater throughout the strong-shock regime than those predicted by Snay. This most likely is an artiface of finite-difference hydrocode calculation.

Comparison of pulse durations

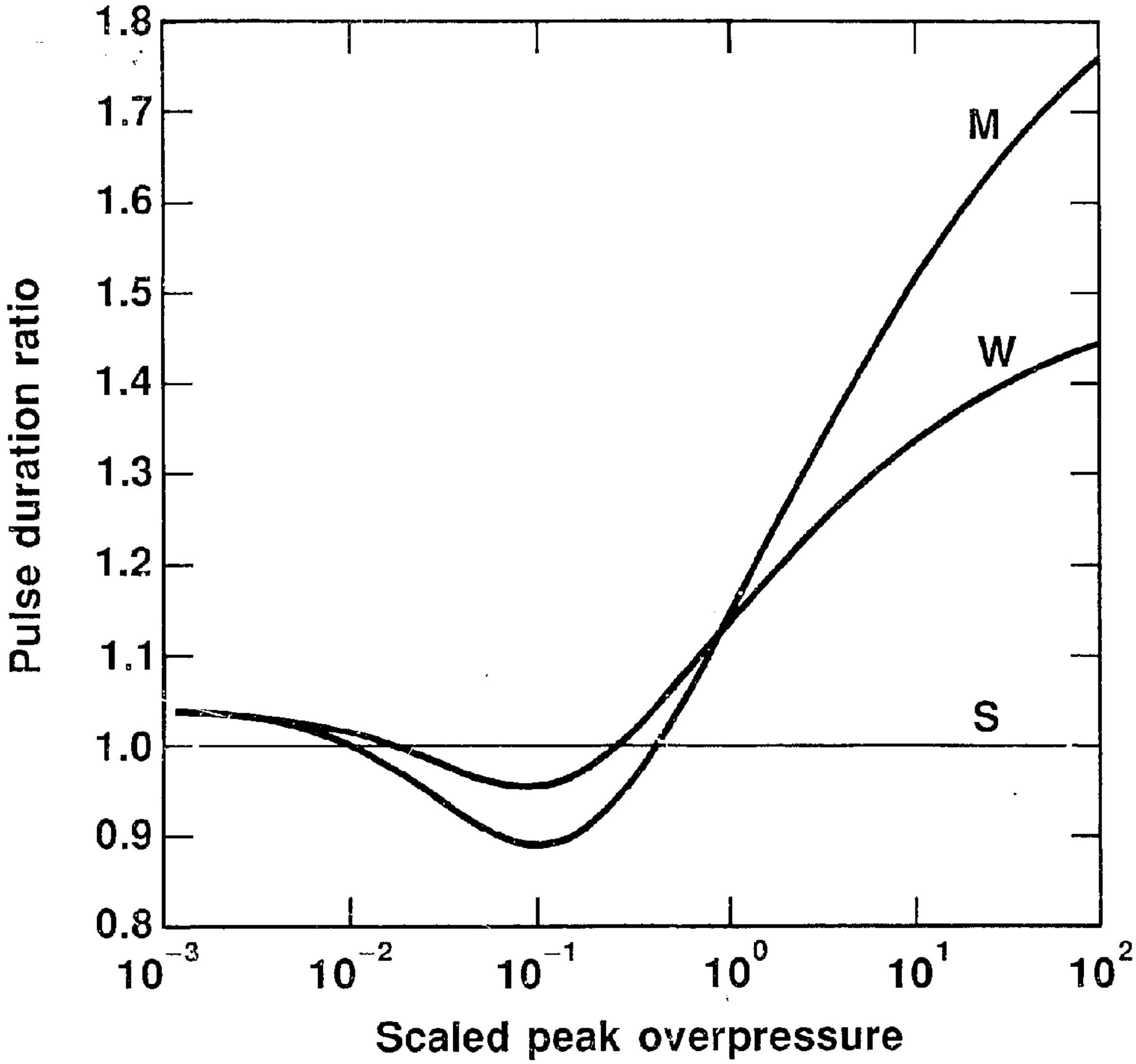

Fig. 20

SUMMARY

This briefing describes the variation in pulse strength and duration as strong and weak spherical shock waves propagate through uniform, homogeneous water from a nuclear explosion. Intrinsic physical scales are introduced, which delineate strong from weak shocks. Elementary non-dimensional interpolation formulas are constructed by using appropriate asymptotic relationships. These interpolation formulas continuously span the entire spatial range from the near-source region out through the far field region of interest for submarine damage prediction. They also could be used to predict initial waveforms for starting propagation calculations in the weak-shock domain, in the absence of more detailed hydrocode input. Finally, results from LASNEX computer simulations of underwater nuclear explosions are compared with the interpolation formulas in order to illustrate the range of applicability of current hydrocodes for doing weak-shock propagation.

Future computational work should focus upon several areas: (A) The present idealistic assumptions, such as constant sound speed and homogeneous, single phase material, should be relaxed. (B) More mesh resolution should be provided where it is needed and determined by the evolution of the steep gradients as the computation develops. This might be accomplished by adaptive mesh refinement or automatic rezoning techniques, which have been designed to optimize the available number of zones. (C) Front tracking may be useful, perhaps even essential, in studying weak-shock propagation, but disentangling the outgoing states is complicated when there are interactions between disturbances or with interfaces. Hybrid methods, which combine advantages of both front tracking and shock capturing, may be preferable.

REFERENCES

[1] M. Kamegai, "Computer Simulation of Underwater Nuclear Events," Lawrence Livermore National Laboratory Report, UCID-20697, September 1986.

[2] M. Kamegai, L. S. Klein, and C. E. Rosenkilde, "Computer Simulation of the Effect of Free Surface Reflection on Shock Wave Propagation in Water," in Shock Waves in Condensed Matter, Y. M. Gupta, ed. (Plenum Press, N. Y. 1986), pp. 673-676.

[3] M. Kamegai, "Computer Simulation of Irregular Surface Reflection of an Underwater Shock Wave," Lawrence Livermore National Laboratory Report, UCID-20701, September 1986.

[4] W. D. Curtis and C. E. Rosenkilde, "Hydrodynamic Attenuation of Weak Shock Waves," J. Acoustical Soc. Am. 77, Supplement 1, Spring 1985, p. S47. (abstract)

[5] B. E. McDonald and W. A. Kuperman, "Time Domain Soltion of the Parabolic Equation including Nonlinearity," Comp. and Maths. with Appls. 11, 843-851(1985).

[6] V. E. Fridman, "The Region of Nonlinear Effects for Intense Sound Pulses in the Ocean," Wave Motion 1, 271-277(1979).

[7] J. H. Ginsberg and C. E. Rosenkilde, "DAA Modal Analysis for Parametric Investigations of Fluid-Structure Interaction in Underwater Shock," Shock and Vibration Bulletin 55, Supplement 3, pp. 25-35, March 1986.

[8] C. E. Rosenkilde and J. H. Ginsberg, "Angle of Incidence Effects for Underwater Shock Using Generic Computational Models," Shock and Vibration Bulletin 55, Supplement 3, pp. 37-57, March 1986.